PNAS RESEARCH ARTICLE | PHYSICS

A stability bound on the T-linear resistivity of conventional metals

Chaitanya Murthy[a], Akshat Pandey[a], Ilya Esterlis[b], and Steven A. Kivelson[a,1]

Contributed by Steven A. Kivelson; received September 28, 2022; accepted December 6, 2022; reviewed by Andrew P. Mackenzie and D.L. Maslov

Perturbative considerations account for the properties of conventional metals, including the range of temperatures where the transport scattering rate is $1/\tau_{\mathrm{tr}} = 2\pi\lambda T$, where λ is a dimensionless strength of the electron–phonon coupling. The fact that measured values satisfy $\lambda \lesssim 1$ has been noted in the context of a possible "Planckian" bound on transport. However, since the electron–phonon scattering is quasielastic in this regime, no such Planckian considerations can be relevant. We present and analyze Monte Carlo results on the Holstein model which show that a different sort of bound is at play: a "stability" bound on λ consistent with metallic transport. We conjecture that a qualitatively similar bound on the strength of residual interactions, which is often stronger than Planckian, may apply to metals more generally.

resistivity bounds | electron–phonon problem | polaronic effects

Significance

Analyses of transport data in metals, both conventional and unconventional, have suggested that the slope of any linear-in-temperature resistivity is bounded from above, leading to many speculative theoretical proposals concerning fundamental bounds on dissipation and thermalization in metals. On the basis of an exact numerical solution of a generic model of the electron–phonon problem, we clearly identify the origin of the bound in conventional metals and associate it with a crossover into a bipolaronic regime when interactions are strong. This result suggests that more broadly, the observed bound may reflect a limit to the interaction strengths between low-energy modes consistent with the stability of a metallic state.

The electrical resistivity of conventional metals varies linearly with temperature T in the regime $T \gtrsim \omega_0$, where ω_0 is a characteristic phonon frequency. The corresponding transport scattering rate extracted via Drude analysis is $1/\tau_{\mathrm{tr}} = \alpha T$ (in units where $\hbar = k_B = 1$). Ambiguities associated with the Drude fit notwithstanding, it was observed that across a wide range of materials, the values of the dimensionless constant α are bounded by a number of order one (1). In conventional Migdal–Eliashberg–Bloch-Grüneisen (MEBG) theory, $\alpha = 2\pi\lambda$, where λ is a suitably defined dimensionless electron–phonon coupling constant which is not a priori bounded. The observed bound is therefore striking and has stimulated considerable theoretical activity, especially insofar as it coincides with a possible bound christened "Planckian" (2) on local equilibration rates in unconventional materials such as the cuprates (3). An attractive feature of this idea is that it might transcend any quasiparticle-based theoretical framework and hence give insight into a set of puzzling phenomena which have been variously identified as "bad metals" (4, 5), "strange metals" (6, 7), "marginal Fermi liquids" (8, 9), etc.

We propose that, in the relevant temperature regime in metals with strong electron–phonon scattering, there is in fact generically a crossover at $\lambda \sim 1$ from metallic to insulating transport, driven by polaron physics. This corresponds to a bound on the slope of the T-linear resistivity—if λ were any larger, the system would no longer be metallic. Our picture comes from Monte Carlo studies of the paradigmatic Holstein model in the limit of zero phonon frequency, $\omega_0 = 0$, and more limited previous results on the breakdown of MEBG theory for $0 < \omega_0 \ll T$ (10–14) (for a comprehensive review, see ref. 12). The results are summarized through a phase diagram in the λ-T plane in Fig. 1 and resistivity curves at various λ in Fig. 2. While the proposed stability bound on λ implies a bound on $1/\tau_{\mathrm{tr}}$ that has the same functional form as the conjectured Planckian bound, the physical origin is entirely different. Because scattering here is entirely elastic, the notion of a bound on thermalization of the electron fluid is irrelevant, whatever its meaning in less well-understood highly correlated materials.*

The Holstein model is at best a caricature of any actual metal and has no direct relevance to more complicated problems in which electron–electron interactions play a central role. Nonetheless, we conjecture that the inferred stability bound is broadly relevant in real materials, with the caveat that the precise value of α at the crossover point beyond which metallic behavior ceases depends on microscopic details. This conjecture rationalizes the otherwise surprising observation that when measured values of λ are tabulated in conventional metals, no values larger than $\lambda \approx 2$ are found (15, 16). Extending this intuition to more general (and less well-understood) problems, we further conjecture that the coefficient α in any metallic system exhibiting a T-linear resistivity can intuitively be associated with the strength of interactions among its low-energy degrees

*Electron–phonon scattering is quasielastic at $T \gg \omega_0$ and entirely elastic in the limit $\omega_0 \to 0$. The fact that the stability bound on λ holds even in this (unphysical) limit emphasizes that it is conceptually unrelated to any bound on thermalization.

Author affiliations: [a]Department of Physics, Stanford University, Stanford, CA 93405; and [b]Department of Physics, Harvard University, Cambridge, MA 02138

Author contributions: C.M., A.P., I.E., and S.A.K. designed research; performed research; analyzed data; and wrote the paper.

Reviewers: A.P.M., Max Planck Institute for Chemical Physics of Solids; and D.L.M., University of Florida.

The authors declare no competing interest.

[1]To whom correspondence may be addressed. Email: kivelson@stanford.edu.

This article contains supporting information online at http://www.pnas.org/lookup/suppl/doi:10.1073/pnas.2216241120/-/DCSupplemental.

Published January 12, 2023.

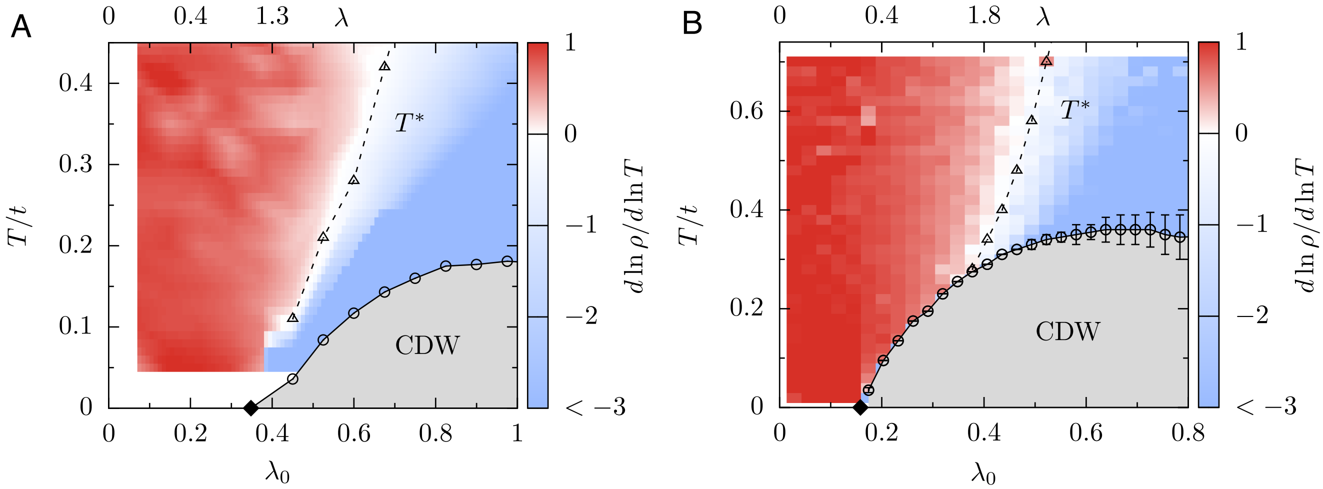

Fig. 1. Transport phase diagram of the 2D (*A*) and 3D (*B*) Holstein model with static phonons as a function of bare (renormalized) electron–phonon coupling λ_0 (λ) and temperature T. The color scale indicates the T dependence of the resistivity ρ, represented as an effective thermal exponent. CDW denotes a (π,π) or (π,π,π) charge density wave insulator. The T^* line is a crossover at which a pseudogap in the single-particle density of states first appears, which also approximately coincides with the crossover from a "metallic" to "insulating" T dependence of the resistivity. The value of the renormalized coupling λ (shown on the upper scale of the figure), which is temperature dependent, is computed at $T = 0.25t$ in 2D and $T = 0.4t$ in 3D. Note that in the deep blue region, the dependence on T is stronger than T^{-3}. In (*A*) the chemical potential for each λ_0 is such that $n(T = 0.25t) = 0.8$, while in (*B*) the density is $n = 1$ throughout the phase diagram. The calculations were done with nonzero next-nearest-neighbor hopping t', with $t' = -0.3t$ in 2D and $t' = -0.2t$ in 3D.

of freedom, and so, a bound on α reflects a bound on this interaction strength consistent with the existence of the metallic state.

Results for the Holstein Model

We consider the Holstein Hamiltonian describing one band of noninteracting electrons coupled to an Einstein phonon,

$$H = \sum_{ij\sigma} t_{ij} c^\dagger_{i\sigma} c_{j\sigma} + \sum_i \left(\frac{p_i^2}{2M} + \frac{1}{2} K x_i^2 \right) + \gamma \sum_{i\sigma} x_i n_{i\sigma}, \quad [1]$$

where $c^\dagger_{i\sigma}$ creates an electron on site i with spin σ, t_{ij} is the hopping matrix element between sites i and j, x_i/p_i are the phonon displacement/momentum on site i, $\omega_0 = \sqrt{K/M}$ is the phonon frequency, and γ is the electron–phonon coupling constant, which couples the oscillator displacement to the total electron density on site i. The important dimensionless parameters are the coupling strength, conventionally defined as $\lambda_0 = \gamma^2 N_0/K$, and the retardation parameter ω_0/E_F, where N_0 is the bare density of states at the Fermi energy, E_F. It is important to distinguish between the bare coupling, λ_0, and the renormalized coupling, λ. The latter is the more physically relevant quantity and is defined in terms of an appropriate average of the inverse of the renormalized stiffness, $\widetilde{K}(\mathbf{q})$, at wavevector $\mathbf{q}$. There are in fact different definitions of λ, corresponding to different averages over $\mathbf{q}$. In our studies, we find that the different commonly used averages give essentially the same value. Common definitions of λ are summarized in *SI Appendix*, section 2.

With some important exceptions, the regime of the Holstein model relevant to conventional metals is $\omega_0/E_F \ll 1$. A representative phase diagram of the model in this limit as a function of λ and T is shown in Fig. 1. At low temperatures, there is generically a superconducting phase for weak to moderate coupling when $T < T_{SC} \sim \omega_0 e^{-1/\lambda}$. (The superconductor does not appear in our phase diagram because we will consider the limit $\omega_0 \to 0$.) There is an insulating charge density wave (CDW) phase for stronger coupling when $T < T_{CDW}$,[†] where for large λ (not shown in the figure) $T_{CDW} \sim t/\lambda$ (11). Qualitatively similar phase diagrams have been derived previously, for instance in refs. 18–20. Here, our principal interest will be in the transport properties in the disordered "high-temperature" regime, where $T > \omega_0$ (and hence $T > T_{SC}$) and $T > T_{CDW}$, but still $T \ll E_F$.

When $T > \omega_0$, the phonons are effectively classical, and so, we will consider a simpler version of Eq. **1** in which we take $M \to \infty$, implying $\omega_0 \to 0$, and study the model via Monte Carlo simulation. Calculations with classical phonons are significantly simpler computationally and also allow for evaluation of dynamical observables without the need for analytic continuation. Moreover, we have previously (10, 11) verified that results for various thermodynamic observables in the temperature range of interest are unchanged if calculations are carried out with finite ω_0. Dividing the Hamiltonian into phonon-only and other terms, $H = H_{ph} + H_e$, the thermal average of any electronic observable $\mathcal{O}$ is given, in the $M \to \infty$ limit, by

$$\langle \mathcal{O} \rangle \propto \int DX\, e^{-\beta H_{ph}[X] + \ln Z_e[X]}\, \mathcal{O}[X], \quad [2]$$

where $Z_e[X] = \mathrm{Tr}\, e^{-\beta H_e[X]}$ is the electronic partition function and $\mathcal{O}[X] = \mathrm{Tr}(\mathcal{O}\, e^{-\beta H_e[X]})/Z_e[X]$ the thermal average of the observable for a given static phonon configuration $X = \{x_i\}$. The integral over X is performed by Monte Carlo sampling. Further details of the algorithm are summarized in ref. 11 and in *SI Appendix*, section 1.[‡]

The data presented here were computed using a 2D square lattice with periodic boundary conditions and linear sizes $L \le 20$ and a 3D cubic lattice with $L \le 14$. We present results for

[†] Our CDW transition temperatures are in agreement with those reported for the 2D and 3D Holstein model with finite ω_0 (17).

[‡] There is an extensive body of work on the problem of itinerant electrons coupled to classical spin degrees of freedom, related to the problem of magnetoresistance in manganites (21). While the numerical techniques are similar to those used here, the physics is distinct. For instance, the fixed-length constraint on the spins implies drastically different transport at elevated temperatures.

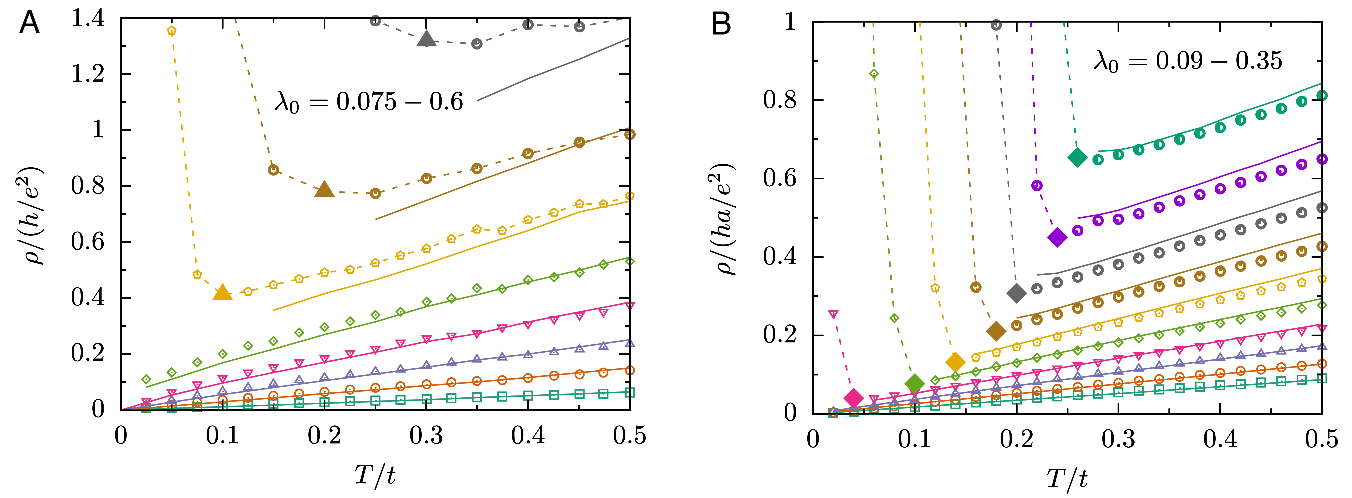

Fig. 2. Resistivity of the 2D (*A*) and 3D (*B*) model versus temperature T for values of the electron–phonon coupling $\lambda_0 = 0.075$–0.6 in steps of 0.075 in 2D, and $\lambda_0 = 0.087$–0.348 in steps of 0.029 in 3D. In the normal metallic (small λ_0) regime, the resistivity is approximately T-linear with zero intercept and a slope that increases (faster than linearly) with λ_0. The high-temperature behavior in the strongly coupled ($\lambda_0 \gtrsim 0.4$ in 2D, $\lambda_0 \gtrsim 0.3$ in 3D) "bad-metallic" regime involves a resistivity that is comparable to or larger than the quantum of resistivity, and although it grows approximately linearly with T, it extrapolates to an increasingly large $T \to 0$ intercept, despite the absence of quenched disorder. Solid lines are the Bloch–Grüneisen (BG) formula using the renormalized λ, which is obtained from the phonon Green's function measured in Monte Carlo. Dashed curves are guides to the eye in those regimes where the BG formula is not a good fit to the data. In (*A*), solid triangles indicate the resistivity at the pseudogap temperature, T^*. In (*B*), solid diamonds indicate the same just above the CDW transition temperature.

the case in which t_{ij} contains nearest-neighbor hopping t and next-nearest-neighbor hopping $t' = -0.3t$ (2D) or $t' = -0.2t$ (3D). In 2D, we have fixed the chemical potential such that the average density is $n(T = 0.25t) = 0.8$.[§] In 3D, we have fixed the average density to one electron per site, $n = 1$, at all T. In the noninteracting limit, $E_F \approx 1.8t$ (2D) and $E_F \approx 3.1t$ (3D). We have verified that none of the results are qualitatively sensitive to the particular choice of parameters or model details. In *SI Appendix*, section 6, we report additional data demonstrating the insensitivity of our results to varying electron density or including explicit phonon anharmonicity.

The main observable of interest is the conductivity, $\sigma(\omega)$, which refers here just to its real part. For a given static phonon configuration X, this is computed as (here $\hbar = 1$):

$$\sigma(\omega; X) = \frac{1}{L^d}\frac{2\pi}{\omega}\sum_{\nu\nu'}[f(E_\nu) - f(E_{\nu'})] \times |\langle\nu|\hat{J}|\nu'\rangle|^2\delta(\omega - E_\nu + E_{\nu'}), \quad [3]$$

where E_ν and $|\nu\rangle$ denote single particle eigenvalues and eigenvectors of $H_e[X]$, $\hat{J}$ is the single-particle current operator, and $f(E) = [1 + \exp(\beta E)]^{-1}$ is the Fermi function. The factor of two accounts for spin. This quantity is then averaged over equilibrium phonon configurations as in Eq. **2**. We denote the average simply as $\sigma(\omega)$, and the resistivity is $\rho = 1/\sigma(0)$. There are subtleties concerning the way the dc and thermodynamic limits are taken, which we discuss in detail in *SI Appendix*, section 3. Our principal findings are summarized in Fig. 1, which shows $d\ln\rho/d\ln T$ through the phase diagram in the (λ_0, T) plane, and in Fig. 2, which plots $\rho(T)$ versus T for various λ_0. The corresponding values of the renormalized coupling λ are also reported in the figures.

Clearly, for $\lambda_0 \gtrsim 0.5$, the low-temperature CDW (a true broken-symmetry insulator) melts to a state with finite but insulating resistivity, to wit $d\rho/dT < 0$. Above a temperature T^*_ρ which, for large λ_0, is roughly the bipolaron binding energy, $T^*_\rho \approx \gamma^2/K$, we find that $d\rho/dT > 0$ again, but with a substantial nonzero extrapolated $T \to 0$ intercept despite the absence of disorder. T^*_ρ approximately coincides with the appearance of a pseudogap in the single-particle density of states, indicated by T^* in our phase diagram (10, 11). The essential observation is that for the range of temperatures we are interested in ($\omega_0 \ll T \ll E_F$), there is a sharp metal-to-insulator crossover in the resistivity at $\lambda \sim 1$ driven by pseudogap formation and hence a bound on the metallic T-linear resistivity.

We stress that this metal-to-insulator crossover is a reflection of local polaron physics and is conceptually unrelated to a low-temperature CDW transition. Where T^* is well above T_{CDW}, the CDW correlation length is small at the crossover. We have also carried out simulations at lower densities where charge ordering is suppressed, yet we find that T^* remains essentially unchanged (*SI Appendix*, section 6). In addition, we can accurately describe the crossover using an approximation that completely neglects correlations between phonon displacements on different sites, as discussed below.

Relation to Theory

On the metallic side of the phase diagram, we find that the conventional MEBG theory captures remarkably well the behavior of thermodynamic observables (11) as well as the dc resistivity. Comparisons of the resistivity between the MEBG theory and Monte Carlo are shown in Fig. 2. (The agreement with MEBG theory in the metallic regime further validates the use of $M \to \infty$ in the Monte Carlo simulations.) A different approach is required for the insulator and crossover region. We have found that modeling the phonons in a "local" approximation as disorder with vanishing correlation length—i.e., ignoring correlations between phonon displacements on different sites—produces reasonable quantitative agreement with the Monte Carlo data.

[§]Above the CDW transition, the density varies weakly with temperature. In the CDW phase, the density approaches $n = 1$; see figure 3 of ref. 11.

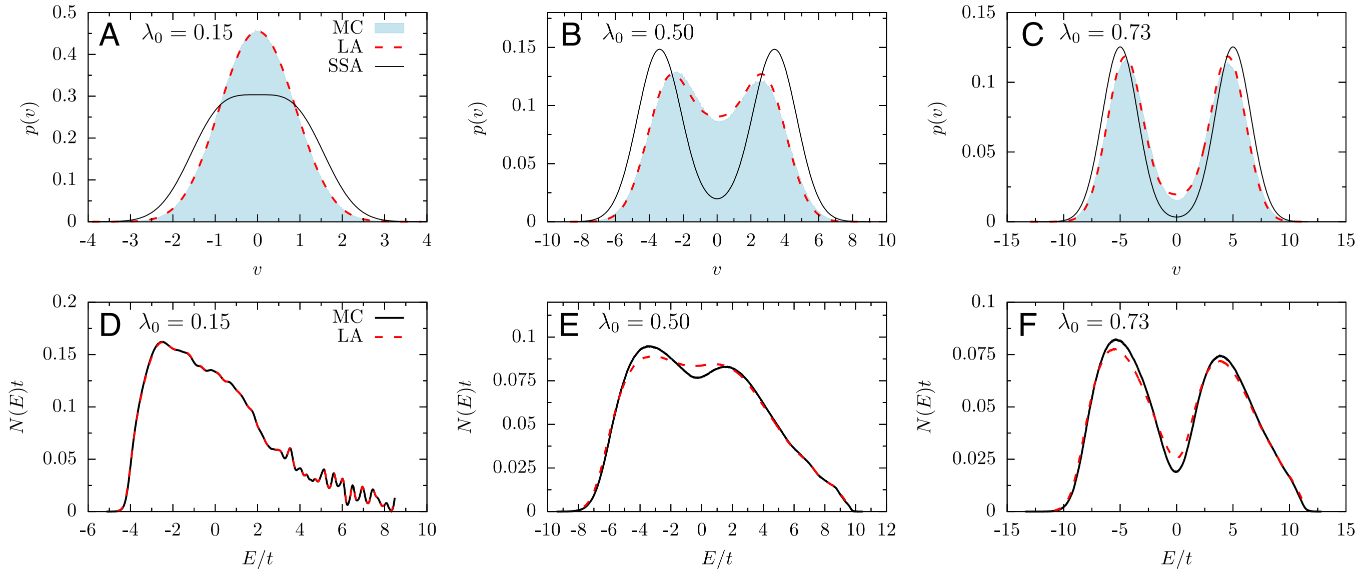

Fig. 3. Distribution of on-site potentials (*A–C*) and electronic density of states (*D* and *E*) in 3D, for values of λ_0 on the metallic side of the phase diagram (*A* and *D*), near the pseudogap crossover (*B* and *E*), and in the insulating regime (*C* and *F*). The temperature is $T = 0.5t$. In *A–C*, we show the on-site distributions from Monte Carlo (MC), a fit to the MC using the local approximation (LA), and the single site approximation (SSA) (*SI Appendix* for more details). The measured distributions are accurately captured by the LA, while the SSA is only qualitatively accurate. *D–F* show the density of states as measured in MC and that obtained from a quenched disorder average using the LA. Data are for $L = 10$; the wiggles in the density of states (especially in *D*) are finite size effects that become less pronounced with increasing *L*.

Formally, the Holstein model with $\omega_0 = 0$ constitutes an annealed disorder problem; see Eq. **2**. The joint probability distribution for the site potentials $v_i = \gamma x_i$ is $P[V] \propto e^{-\beta H_{\rm ph}[V] + \ln Z_{\rm e}[V]}$, where $Z_{\rm e}[V] = {\rm Tr}\, e^{-\beta H_{\rm e}[V]}$ is the electronic partition function computed for the given potential realization $V = \{v_i\}$. In general, $P[V]$ is a complicated nonlocal T-dependent object. We would like to approximately replace it with a local disorder distribution $P_{\rm loc}[V] = \prod_i p(v_i)$. The on-site distributions $p(v_i)$, in turn, can be extracted from the Monte Carlo data, with representative results shown in Fig. 3.

We can obtain a crude representation of $p(v)$ by considering the statistical properties of a single isolated site (no hopping), for which we can compute the phonon distribution $p_{\rm ss}(v)$ exactly as a function of the chemical potential μ and temperature T:

$$p_{\rm ss}(v) = p_0 \left[e^{-\frac{(v-U_0)^2}{2UT}} + 2y e^{-\frac{v^2}{2UT} - \frac{U_1}{2T}} + y^2 e^{-\frac{(v+U_0)^2}{2UT}} \right], \qquad [4]$$

where $U_0 = U_1 = U \equiv \gamma^2/K$ is the characteristic bipolaron binding energy, $y = e^{\mu/T}$ is the electron fugacity ($y = 1$ when there is on average one electron per site), and p_0 is the requisite normalization factor. This approximation becomes better the deeper we are in the insulating phase, i.e., the more localized the electronic states in a typical realization of V are. In the intermediate range of λ of primary interest here, $p(v)$ deviates substantially from $p_{\rm ss}(v)$, but it can be well parameterized by the same functional form with U_0 and U_1 treated as T and λ dependent parameters; we therefore do this when making direct comparisons with the numerical data. One can then calculate electronic observables in realizations of V and perform a quenched average using $P_{\rm loc}[V]$.

Roughly speaking, $p_{\rm ss}(v)$ contains peaks at $v = \pm U$, each of width $\sqrt{TU}$. At strong coupling ($\lambda_0 > 0.5$), when U is larger than both the unperturbed bandwidth and T, the disorder distribution is bimodal, and the density of states itself splits into two peaks, such that the integrated density of states per spin in the low-energy peak is $n/2$.[¶] The chemical potential thus automatically lies in the pseudogap between them—this contrasts with the case of a corresponding problem with quenched disorder where the chemical potential is an independent quantity that is not generically tied to the pseudogap. This band splitting captures the binding of electrons into bipolarons. The states deep in the pseudogap are strongly localized.

However, even at strong coupling, increasing T beyond U makes the disorder distribution single-peaked, and there is no pseudogap. Although the effective disorder is relatively strong here, one can crudely understand the observed T dependence of the resistivity with perturbative reasoning—assuming that the scattering rate (and hence the resistivity itself) is proportional to the mean-square disorder potential, $\overline{(v_i - \bar{v})^2} \sim U^2 + UT$. This accounts both for the observed linear-in-T growth and the large extrapolated $T \to 0$ intercept of ρ in Fig. 2 in this range of T and λ_0.

Ultimately, the observed metal-insulator crossover apparent in the Monte Carlo data occurs for two closely intertwined reasons: the band splitting causes a depression in the density of states (pseudogap) at the Fermi level, and these states become more and more localized. The single-site approximation captures qualitatively the essential physics of the crossover and is quantitatively accurate at sufficiently strong coupling. Over a much broader range of couplings, we are still able to fit the distribution of site energies measured in the Monte Carlo data by treating U_0 and U_1 in Eq. **4** as adjustable parameters. Observables computed using the resulting $P_{\rm loc}[V]$ agree reasonably well with their Monte Carlo values throughout the phase diagram (except, of course, in or very near the CDW phase). Representative results are shown in Fig. 3.

[¶] In strong coupling and ignoring thermal broadening, the effective disorder distribution is that of a binary alloy—with energy $-U$ on the "bipolaron sites" and energy $+U$ on the remaining sites. Manifestly, the concentration of bipolaron sites is $n/2$. When $2U$ is larger than the bandwidth, by the spectral localization theorem (22), this would give rise to a hard gap and an integrated density of states per spin in the lower band precisely equal to $n/2$. Thermal broadening turns this gap into a pseudogap, which survives even when $2U$ is somewhat less than the bandwidth.

Note that for large λ, the local approximation is equivalent to previous results obtained using dynamical mean field theory (DMFT) for the same problem (18, 19, 23). Indeed, the DMFT results appear to agree—at least qualitatively—with our Monte Carlo results, even at small λ where the naive single-site approximation (with $U_0 = U_1 = U$) fails.

Stability Bounds

While the results obtained concern a simplified model, we expect the qualitative and even the rough quantitative aspects of the results to apply in realistic circumstances in which electron–phonon coupling is strong. There are a number of material systems which, as a function of pressure, strain, doping concentration, or even photoexcitation, can be tuned from a metallic or superconducting to an insulating CDW ground state. To the extent that these low-temperature phase transitions reflect changes in the strength of the electron–phonon coupling λ, a corresponding crossover should be expected at elevated temperature in the "normal state" from metallic T dependence on the small λ side of the crossover to increasingly insulating T dependence on the large λ side. Moreover, at the crossover, the scattering rate should be $1/\tau \sim 2\pi T$ (corresponding to $\lambda \sim 1$). A systematic comparative study of such crossovers in a variety of materials would be an interesting way to test the relevance of the present studies. Examples of systems which at least superficially exhibit some aspects of this expected behavior include certain organics (24, 25) and BPBO (26).

More generally, the appeal of invoking a Planckian bound $1/\tau_{\mathrm{eq}} \leq 2\pi T$ in relation to transport is the hope that it gives a way to understand the origin of T-linear resistivity in a variety of unconventional metallic systems. A priori, the above discussion is applicable only to conventional metals, where the physics of the T-linear resistivity has been well understood for decades and the main insight we have to offer concerns why larger values of α are never observed. However, one can speculate that there is a broader sense in which the present results may inform the discussion of less well-understood metallic systems as well (27).

It is certainly conceivable that a T-linear resistivity can arise in a semiclassical regime in which electrons scatter from another form of collective soft mode of a system, other than a phonon. Here, the same considerations we have explored above apply more or less directly.

More generally, it is a common (not necessarily universal) feature of quantum systems that strong interactions among propagating particles reduce itineracy. Thus, it is reasonable to suppose—in the absence of disorder—that the resistivity (or more directly $1/\tau_{\mathrm{tr}}$) is a measure of the strength of the residual interactions between low-energy degrees of freedom. At the same time, there is general sense in which strong interactions lead to a reorganization of the effective low energy degrees of freedom. This can be made precise in some systems in which there is an explicit transformation relating a set of interacting "microscopic" variables to a set of dual degrees of freedom, such that when the former is strongly interacting, the latter is weakly interacting, and vice versa. But the underlying physical intuition is likely more broadly valid—that there is a rough maximum strength of an appropriate dimensionless measure of the effective interactions consistent with a metallic state.

Thus, we conclude with the conjecture that there is a general stability bound on the magnitude of the resistivity of any metallic state—one that often is much more restrictive (and hence more significant) than the putative Planckian bound, as we explain in *SI Appendix*, section 4. Where $1/\tau_{\mathrm{tr}} \approx \alpha T$, even when this is not directly attributable to electron–phonon scattering, it is reasonable to suppose that α is the correct dimensionless measure of the interaction strength and so is bounded by these considerations.[#] Where $1/\tau_{\mathrm{tr}}$ has a more complicated T dependence, it requires further analysis to relate its magnitude to a dimensionless interaction strength. However, in some cases, such a relationship can be established on other grounds. For example, at low T, electron scattering from long-wavelength acoustic phonons dominates the resistivity of many metals, such that $1/\tau_{\mathrm{tr}} \sim \lambda_D T^5/\omega_D^4$ where ω_D is the Debye frequency, which can be independently determined. Thus, a bound on λ_D implies a corresponding bound on the resistivity. One can also consider extracting an estimate of the strength of the residual interactions from dimensional analysis, as $\lambda_{\mathrm{eff}} \sim 1/\Omega\tau_{\mathrm{tr}}$, where Ω is a characteristic energy scale in the problem. In most metals, a lower bound on λ_{eff} can be obtained by taking $\Omega = E_F$ since typically E_F is the largest characteristic scale. This leads to a somewhat different perspective on the familiar Ioffe-Regel limit, usually stated as $E_F\tau_{\mathrm{tr}} \sim k_F\ell \gtrsim 1$.

In summary, we propose that, while the precise way in which it plays out can vary depending on specifics, there is an approximate stability bound on the maximum magnitude of an appropriate dimensionless measure of the transport scattering rate in all clean metallic systems.[‖]

Data, Materials, and Software Availability. There are no data underlying this work.

ACKNOWLEDGMENTS. We gratefully acknowledge conversations with Kamran Behnia, Erez Berg, Sankar Das Sarma, Luca Delacrétaz, Matthew Fisher, Jim Freericks, Sarang Gopalakrishnan, Tarun Grover, Nigel Hussey, Prashant Kumar, Andy Mackenzie, Chetan Nayak, Brad Ramshaw, John Sous, and especially with Sean Hartnoll. This work was supported in part by the Gordon and Betty Moore Foundation's EPiQS Initiative through GBMF8686 (C.M.), the Stanford Graduate Fellowship (A.P.), NSF award DMR-2038011 (I.E.), and NSF grant No. DMR-2000987 at Stanford (S.A.K.). C.M. also acknowledges the hospitality of the Kavli Institute for Theoretical Physics, supported by the National Science Foundation under grant No. NSF PHY-1748958.

[#] For example, in ref. 28, the transport properties of the Hubbard model with intermediate U were analyzed using the dynamical mean field theory (DMFT), with particular focus on an intermediate temperature regime $T_{\mathrm{FL}} < T < T_{\mathrm{MIR}}$, where T_{FL} is a temperature below which Fermi liquid theory applies and T_{MIR} is the temperature above which the resistivity exceeds the quantum of resistance. In this regime, the resistivity is found to be approximately linear in T with a slightly negative extrapolated value at $T \to 0$. An interpretation of the results in terms of highly dressed "resilient quasiparticles" is shown to account for the behavior qualitatively, where a suitably defined transport scattering rate depends on hole-doping and T (and, presumably, U/t) but is "at most comparable to T." This model is conceptually unrelated to the electron–phonon problem we have analyzed, but it is plausible that a related stability bound is the explanation for the apparent bound on $1/\tau_{\mathrm{tr}}$.

[‖] To avoid misunderstanding, we review the fine print on this proposal: The proposed bound is approximate in the sense that it involves a dimensionless number of order one that can depend on microscopic details. However, it appears to be difficult to find physically reasonable circumstances in which this number is substantially larger than 1. It is only indirectly related to a resistivity bound, in the sense that ρ is proportional to $1/\tau_{\mathrm{tr}}$. As already discussed, determining the appropriate energy scale to relate the dimensional $1/\tau_{\mathrm{tr}}$ to a dimensionless coupling constant generally involves additional analysis, but in circumstances in which the scattering rate is T-linear, the correct dimensionless quantity is $1/\tau_{\mathrm{tr}}T$.

1. J. A. N. Bruin, H. Sakai, R. S. Perry, A. P. Mackenzie, Similarity of scattering rates in metals showing T-linear resistivity. *Science* **339**, 804–807 (2013).
2. J. Zaanen, Why the temperature is high. *Nature* **430**, 512–513 (2004).
3. S. A. Hartnoll, A. P. Mackenzie, Colloquium: Planckian dissipation in metals. *Rev. Mod. Phys.* **94**, 041002 (2022).
4. V. J. Emery, S. A. Kivelson, Superconductivity in bad metals. *Phys. Rev. Lett.* **74**, 3253–3256 (1995).
5. N. E. Hussey, K. Takenaka, H. Takagi, Universality of the Mott-Ioffe-regel limit in metals. *Philos. Mag.* **84**, 2847–2864 (2004).
6. J. Zaanen, Planckian dissipation, minimal viscosity and the transport in cuprate strange metals. *SciPost Phys.* **6**, 061 (2019).

7. S. A. Hartnoll, Theory of universal incoherent metallic transport. *Nat. Phys.* **11**, 54–61 (2015).
8. C. M. Varma, Colloquium: Linear in temperature resistivity and associated mysteries including high temperature superconductivity. *Rev. Mod. Phys.* **92**, 031001 (2020).
9. C. M. Varma, P. B. Littlewood, S. Schmitt-Rink, E. Abrahams, A. E. Ruckenstein, Phenomenology of the normal state of Cu-O high-temperature superconductors. *Phys. Rev. Lett.* **63**, 1996 (1989).
10. I. Esterlis *et al*., Breakdown of the Migdal-ELiashberg theory: A determinant quantum Monte Carlo study. *Phys. Rev. B* **97**, 140501 (2018).
11. I. Esterlis, S. A. Kivelson, D. J. Scalapino, Pseudogap crossover in the electron-phonon system. *Phys. Rev. B* **99**, 174516 (2019).
12. A. V. Chubukov, A. Abanov, I. Esterlis, S. A. Kivelson, Eliashberg theory of phonon-mediated superconductivity–when it is valid and how it breaks down. *Ann. Phys.* **417**, 168190 (2020).
13. J. Bauer, J. E. Han, O. Gunnarsson, Quantitative reliability study of the Migdal-Eliashberg theory for strong electron-phonon coupling in superconductors. *Phys. Rev. B* **84**, 184531 (2011).
14. A. S. Alexandrov, Breakdown of the Migdal-ELiashberg theory in the strong-coupling adiabatic regime. *EPL (Europhys. Lett.)* **56**, 92 (2001).
15. P. B. Allen, "The electron-phonon coupling constant λ" in *Handbook of Superconductivity*, C. P. Poole Jr, Ed. (Academic Press, New York, 1999), pp. 478–483.
16. P. B. Allen, R. C. Dynes, Transition temperature of strong-coupled superconductors reanalyzed. *Phys. Rev. B* **12**, 905 (1975).
17. B. Cohen-Stead *et al*., Langevin simulations of the half-filled cubic Holstein model. *Phys. Rev. B* **102**, 161108 (2020).
18. A. J. Millis, R. Mueller, B. I. Shraiman, Fermi-liquid-to-polaron crossover. I. General results. *Phys. Rev. B* **54**, 5389 (1996).
19. S. Ciuchi, F. De Pasquale, Charge-ordered state from weak to strong coupling. *Phys. Rev. B* **59**, 5431 (1999).
20. S. Fratini, S. Ciuchi, Displaced drude peak and bad metal from the interaction with slow fluctuations. *SciPost Phys.* **11**, 039 (2021).
21. E. Dagotto, T. Hotta, A. Moreo, Colossal magnetoresistant materials: The key role of phase separation. *Phys. Rep.* **344**, 1–153 (2001).
22. H. Ehrenreich, L. M. Schwartz, "The electronic structure of alloys" in *Solid State Physics* (Elsevier, 1976), vol. 31, pp. 149–286.
23. J. K. Freericks, M. Jarrell, D. J. Scalapino, Holstein model in infinite dimensions. *Phys. Rev. B* **48**, 6302 (1993).
24. H. Ito, T. Ishiguro, M. Kubota, G. Saito, Metal-nonmetal transition and superconductivity localization in the two-dimensional conductor κ-(bedt-ttf) 2 cu [n (cn) 2] cl under pressure. *J. Phys. Soc. Jpn.* **65**, 2987–2993 (1996).
25. P. Limelette *et al*., Mott transition and transport crossovers in the organic compound κ-(b e d t- t t f) 2 c u [n (c n) 2] c l. *Phys. Rev. Lett.* **91**, 016401 (2003).
26. S. Uchida, K. Kitazawa, S. Tanaka, Superconductivity and metal-semiconductor transition in BaPb1-xBixO3. *Phase Transit.* **8**, 95–128 (1987).
27. R. A. Cooper *et al*., Anomalous criticality in the electrical resistivity of La2-x Sr x CuO4. *Science* **323**, 603–607 (2009).
28. X. Deng *et al*., How bad metals turn good: Spectroscopic signatures of resilient quasiparticles. *Phys. Rev. Lett.* **110**, 086401 (2013).